

Principal Component Analysis for Equation Discovery

Caren Marzban^{1,2*}, Ulvi Yurtsever³, Michael Richman⁴

¹ Applied Physics Laboratory, ² Department of Statistics
Univ. of Washington, Seattle, WA 98195 USA

³ MathSense Analytics, 1273 Sunny Oaks Circle, Altadena, CA, 91001, USA

⁴ School of Meteorology, University of Oklahoma, Norman, OK 73072, USA

Abstract

Principal Component Analysis (PCA) is one of the most commonly used statistical methods for data exploration, and for dimensionality reduction wherein the first few principal components account for an appreciable proportion of the variability in the data. Less commonly, attention is paid to the last principal components because they do not account for an appreciable proportion of variability. However, this defining characteristic of the last principal components also qualifies them as combinations of variables that are constant across the cases. Such constant-combinations are important because they may reflect underlying laws of nature. In situations involving a large number of noisy covariates, the underlying law may not correspond to the last principal component, but rather to one of the last. Consequently, a criterion is required to identify the relevant eigenvector. In this paper, two examples are employed to demonstrate the proposed methodology; one from Physics, involving a small number of covariates, and another from Meteorology wherein the number of covariates is in the thousands. It is shown that with an appropriate selection criterion, PCA can be employed to “discover” Kepler’s third law (in the former), and the hypsometric equation (in the latter).

Keywords: Equation Discovery, Knowledge Discovery, Data Mining, Principal Components Analysis.

*Corresponding Author: marzban@stat.washington.edu

1 Introduction

Given data on a number of variables, it is often desirable to determine whether some of the variables are related to one another in a useful manner. The use may be for dimensionality reduction, prediction purposes, or for discovering a law of nature. Inferring and understanding structure in large data sets has been an active area of research. Although it has been called by various names, Knowledge Discovery in Data bases, Data Mining, Deep Learning, and Equation Discovery are some of common names (Bergen, et al. 2019; Bongard and Lipson 2007; Grundner et al. 2023; Hoerl, Snee, and De Veaux 2014; Kamath 2001; Kratzert et al. 2019; Kurgan and Musilek 2006; Langley 1981; Marzban and Yurtsever 2011; 2017; Schmidt and Lipson 2009; Song et al. 2023; Wang 1999; Xu and Stalzer 2019; Yu and Ma 2021; Zanna and Bolton 2020; Zhang and Lin 2018). A subset of these works aims to discover - from data - physical laws of nature in terms of relatively simple algebraic equations. For example, the work of Bongard and Lipson (2007), Schmidt and Lipson (2009), and Xu and Stalzer (2019) is based on a symbolic regression approach wherein a space of compact algebraic expressions is searched for an expression that fits the data. One of the most recent works explores automatic determination of the number of state variables, and what they may be, directly from video streams (Chen et al. 2022). The underlying methods are wide-ranging, but Camps-Valls et al. (2023) provides a summary and taxonomy.

The equation discovery methods consider a wide range of equation types, including linear, nonlinear, differential, and partial differential. Although a wide range of scientific fields is examined in these works, Meteorology is not prominently represented among them. Consequently, one purpose of the present article is to consider a demonstration of equation discovery that is familiar to meteorologists. That said, the aim is not to produce a review article, but rather to propose yet another equation discovery method, specifically one that is based on a technique commonly employed in meteorology, namely Principal Component Analysis (PCA), often referred to as Empirical Orthogonal Functions.

One key observation underlying the proposed approach is that a useful relationship between variables will manifest itself as some function of the variables that is constant across the cases in the data. For example, in a data set involving the gravitational force (F) between two objects with masses M and m , separated by a distance r , Newton's law of universal gravitation, $F = GMm/r^2$, would be manifested as $Fr^2/(Mm) = G$, where G is the gravitational constant. In a practical setting, the data on the variables F, M, m, r are subject to "noise," as a result of which the specific combination $Fr^2/(Mm)$ will not be exactly equal to the value of G . In passing, note that the nonlinear equation $Fr^2/(Mm) = G$ can be rendered linear by examining the logarithm of the variables.

The question of whether a certain combination of variables is useful is central to the method of PCA (Hotelling 1933; Jolliffe 2002; Lorenz 1956; Wilks 2019). The most common application of PCA is to identify the most-varying combinations of variables. Consequently, PCA is most often employed for dimensionality reduction, because the combinations with the largest variability encapsulate the information in the data with fewer variables (at least, if the number of variables is less than the number of cases - a condition assumed throughout

this work). PCA in its most common form leads to a set of variable combinations - called Principal Components (PC) - equal in number to the original set of variables, that can be rank-ordered in terms of the amount of the variability explained by each. As such, a subset of PCs consisting of the highest-ranking PCs summarizes the data with fewer variables. The variance explained by each PC, and the coefficients of variables in each PC - often called loadings - are given by the eigenvalues and eigenvectors, respectively, of the sample covariance matrix. In situations where the variables have significantly different variances, it is common practice to examine the eigendecomposition of the correlation matrix.

The second key observation for the proposed method is as follows: Given that equation discovery involves finding combinations of variables that are constant, PCA is appropriate because the lowest-ranking PCs are combinations with the lowest variability. Situations in which the focus of PCA is on the lowest-ranking combinations have been described, and are often referred to as “Last PCA,” or “Least PCA” (Gertler and Cao 2005; Huang 2001; Jolliffe 2002; Jolliffe and Cadima 2016; Rolle 2002; Zlobina and Zhurbin 2020). Although in one of the examples considered here, the relevant equation does in fact appear in the last eigenvector, in general the existence of sampling variability (i.e., noise) implies that the equation of interest may be associated not with the last eigenvector but with one of the last eigenvectors. Indeed, some number of the last eigenvectors are often degenerate, i.e., have equal eigenvalues (Anderson 1963; North et al. 1982). Moreover, it is possible that the data encapsulate multiple laws, or no laws, at all. Although there exist numerous methods for assessing how many of the highest-ranking PCs ought to be saved (Ibebuchi and Richman 2023; Wilks 2016), not only such methods do not exist for lowest-ranking PCs, but more importantly, the identification of relevant PCs requires consideration of physical significance in addition to statistical significance. Therefore, the identification of the relevant eigenvector(s) calls for some sort of a selection criterion, which will be discussed here. With that understanding, henceforth, the “last” eigenvector refers to one of the last eigenvectors.

In short, therefore, an approach to the discovery of equations entails performing PCA on data, and identifying the last PC. That specific combination is, then, the most constant (i.e., least variable) combination of the variables. And the numerical value of that constant can be estimated by the sample mean of the data projected onto the last PC (often called PC score). Another advantage of employing PCA for equation discovery is that PCA treats all variables on the same footing, unlike regression, where the variables must be divided into two sets - predictors and response(s).

Here, such a PCA-based equation discovery method is presented. The outline of the paper is as follows: The Method section provides a high-level presentation of the proposed methodology; this section also includes a subsection wherein a formula is derived relating PCA loadings to parameters of the underlying equation; details of this derivation are contained in the Appendix. Two examples are then considered where further details of the proposed method are revealed. The second example proposes a selection criterion for the last PC, appropriate for situations where the variables are spatial fields - common in Meteorology. The paper ends with a summary of the conclusions, and a discussion of the limitations and generalizations of the method.

2 Method

Given data on p variables, there are several ways of discovering underlying relationships. At the simplest level, one can simply examine the correlation coefficient between all pairs of variables. If, however, one is interested in a relationship that involves multiple variables, then at the broadest level, the methods of choice are regression and PCA. For the specific purpose of equation discovery, the main disadvantage of the former is that it requires the specification of a response variable, or a set of response variables, which *a priori* may be unknown. That said, the main advantage of regression is that the parametric form of regression models naturally aligns with many laws of nature. For example, fitting a regression model of the type $y = \alpha + \beta x + \epsilon$ to data on acceleration x , and force y , will readily “discover” $F = ma$, with the regression coefficient β estimating mass m . Alternatively, one may fit the regression model $y = \alpha + \beta x + \epsilon$ to data on the logarithm of acceleration and force, in which case the parameter α would estimate the logarithm of m , and the slope parameter β would be approximately 1. This natural alignment of the regression line and physical laws is a consequence of the fact that the regression line is designed to estimate the conditional mean of y , given x .

By contrast, the parameters in the PCA line $y = a + bx$ cannot be readily identified with physical parameters, because the PCA line is not designed to estimate the conditional mean of y , given x . Instead, it is designed such that its slope points in the direction of maximum variability.¹ However, the main advantage of PCA is that it treats all variables on the same footing, without requiring the separation of variables into responses and predictors. As shown in the next section, it is possible to find analytic, closed-form expressions that relate the parameters of the PCA line to those of the regression line. Therefore, for the purpose of equation discovery it is more natural to use PCA first, and then use the analytic formulas of the next section to infer the parameters of the regression line, i.e., the parameters that naturally align with physical parameters.

2.1 From PCA to Regression

Most often, PCA involves an eigendecomposition of either the covariance or the correlation matrix (although exceptions do exist, e.g., Elmore and Richman 2001). For demonstration purposes consider a data set involving only two variables, x and y . Although the assumption of normality is required only for assessing the statistical significance of the results, for convenience assume that the data follow a bivariate normal distribution with mean parameters μ_x, μ_y , variance parameters σ_x^2, σ_y^2 , and correlation parameter ρ . The covariance matrix can then be written as

$$\Sigma = \begin{pmatrix} \sigma_x^2 & \rho \sigma_x \sigma_y \\ \rho \sigma_x \sigma_y & \sigma_y^2 \end{pmatrix}. \quad (1)$$

¹It can be shown that the PCA line minimizes the sum-square of the **shortest** distances between the data and the line.

The two eigenvectors of Σ can be found to be

$$\begin{pmatrix} 1 & 1 \\ A_+ & A_- \end{pmatrix}, \quad (2)$$

where $A_{\pm} = A \pm \sqrt{1 + A^2}$, and $A = \frac{1}{2\rho}(\frac{\sigma_x}{\sigma_y} - \frac{\sigma_y}{\sigma_x})$. In practice, all of these distribution parameters are estimated by their sample analogs. These two eigenvectors define the direction (slope) of two PCA lines. The eigenvector with the larger eigenvalue points in the direction of maximum variability, and the second eigenvector is orthogonal to the first one. The y-intercept of the lines is fixed by the criterion that the line must go through the point (μ_x, μ_y) . In short, the equations of the PCA lines are $y = a + bx$, with $b = A_{\pm}$. A formula for the y-intercept is also available, but is not given here because the slope parameter is the only parameter of interest.

Figure 1 shows an instance of data (circles) from a bivariate normal with parameters $\mu_x = 0, \mu_y = 10, \sigma_x^2 = 2, \sigma_y^2 = 3, \rho = 0.8$. The two red lines denote the PCA lines. For comparison, the regression line is also shown (in green).

As mentioned previously, the slope that is more relevant to equation discovery is that of the regression line. Given that the slope of the regression line is $\beta = \rho \frac{\sigma_y}{\sigma_x}$, it is easy to show that

$$\beta = \frac{1}{2}[-B\rho^2 \pm \sqrt{B^2\rho^4 + 4\rho^4}], \quad (3)$$

where $B = (b - \frac{1}{b})$, and b denotes the slope of the PCA lines, i.e., A_{\pm} .

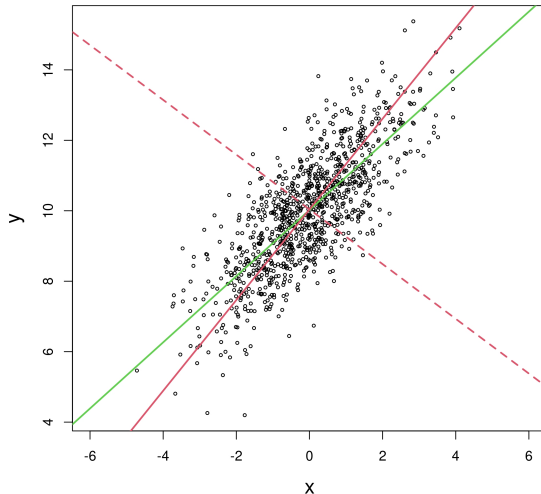


Figure 1. A demonstration of the PCA lines (in red), and the regression line (in green).

As seen in Figure 1, for sufficiently strong correlation between the variables, the PCA line corresponding to the largest eigenvalue is close to the regression line, and the PCA line with the smallest eigenvalue is orthogonal to the regression line. Therefore, in such situations the loadings can be used directly to infer an underlying law, without use of Eq. 3. Example

1 (below) demonstrates this scenario. However, more generally (as in Example 2), Eq. 3 will be used to estimate the parameters of the underlying law.

3 Examples

To demonstrate the above methodology for equation discovery, two examples are considered - one from Physics and Astronomy, and one from Atmospheric Sciences. The rationale for the specific choice of the examples is as follows: First, to illustrate the generality of the methodology, the examples are taken from different fields. Second, Example 1 involves a small number of variables and a small sample size - 5 and 8, respectively. The goal is to show that the last eigenvector does in fact correspond to a known physical law, namely Kepler’s third law. By contrast, the second example involves several hundred covariates because three variables are observed at hundreds of grid points across space. In such a situation the last eigenvector may not play an important role at all, because it is possible to construct linear combinations that have even less variability than the combination corresponding to the law. Therefore, it is necessary to introduce a criterion for identifying the specific eigenvector corresponding to the underlying law, which in the second example is the hypsometric equation.

The task of identifying one of the last eigenvectors that represents a law is not dissimilar to that of selecting some number of the largest eigenvalues that adequately summarize the data with fewer variables. The latter has been studied extensively (Jolliffe 2002), and has given rise to a number of commonly used criteria. One criterion is to select a sufficiently large number of the eigenvectors with the largest eigenvalues that explain some specified percentage of the total variability. Another criterion is to select the eigenvectors up to that corresponding to the “elbow” in the scree plot (Dmitrienko, Chuang-Stein, and D’Agostino 2007). Other criteria are based on statistical significance (Cattell 1966; Wilks 2016). Furthermore, Ibebuchi and Richman (2023) point out that none of these criteria are based on physical considerations of whether a given PC ought to be kept. In short, there does not exist a universal criterion that leads to a unique number of eigenvectors that adequately summarize the data - a situation arising in the present application, as well. Here, a criterion for selecting the physically relevant eigenvector is introduced in Example 2.

3.1 Example 1

Consider Kepler’s third law of planetary motion $\frac{G(M+m)T^2}{a^3} = 4\pi^2$, where G denotes Newton’s gravitational constant, M and m denote the masses of the Sun and of the orbiting planet, and T and a , b denote the period and the semi-major and semi-minor axes of the planet’s elliptical orbit, respectively. If this law were to be discovered empirically, the data would involve 8 observations (for 8 planets) of the variables a, b, m, M, T . The semi-minor axis b has been included, allowing for the possibility that the underlying relationship involves both the semi-major and semi-minor axes. Note that for the solar system M — the central solar

Table 1: Data for the solar system.

Planet	$a(\times 10^{10}m)$	$b(\times 10^{10}m)$	$m(10^{24}Kg)$	$T(Sec)$
Mercury	5.852857	5.727818	0.3244425	7605382
Venus	10.81012	10.80988	4.861260	19407924
Earth	14.95104	14.94896	5.975000	31557600
Mars	22.82995	22.73016	0.6387275	59359846
Jupiter	77.82562	77.73441	1902.141	374336251
Saturn	142.7208	142.4993	569.4175	929623781
Uranus	287.0700	286.7501	87.11550	2651311764
Neptune	449.5683	449.5517	103.1285	5200313789

Table 2: The PCs and the corresponding eigenvalues of PCA performed on the variables a, b, m, M, T .

	PC	eigenvalue
1	$(ab)^2 T^3 m^4$	18.42139
2	$(ab)^2 T^3 / m^4$	2.509082
3	$(a/b)^3$	0
4	$(ab)^3 / T^4$	0
5	M	0

mass for all planetary orbits — is a constant, $M = 1.986616 \times 10^{30}(Kg)$, and $M \gg m$ for any of the planets (for Jupiter $m/M \approx 10^{-3}$). Therefore, in this work Kepler’s law can be taken to be in the form $\frac{GMT^2}{a^3} = 4\pi^2$. The data are shown in Table 1.

Given that PCA involves linear combinations, it is necessary to perform PCA on the logarithm of data. In this log-space, Kepler’s law becomes $2 \log T - 3 \log a = \text{constant}$. Performing PCA on the data shown in Table 1 yields the eigenmatrix shown on the left in Eq. (4), with the columns denoting the eigenvectors, and the rows corresponding to the variables a, b, m, M , and T , respectively. These eigenvectors are orthonormal, but they can be “normalized” differently (as discussed in the discussion section) to expose the underlying near-integer values (right side of Eq. 4). For example, it follows that the first PC involves $a^{2.00} b^{2.01} m^{3.83} M^{0.00} T^{3.00}$.

$$\begin{pmatrix} -0.36 & 0.33 & 0.72 & -0.50 & 0 \\ -0.36 & 0.33 & -0.70 & -0.53 & 0 \\ -0.68 & -0.73 & 0.00 & 0.00 & 0 \\ 0.00 & 0.00 & 0.00 & 0.00 & 1 \\ -0.53 & 0.49 & -0.01 & 0.69 & 0 \end{pmatrix} \sim \begin{pmatrix} 2.00 & 2.00 & 1.00 & 3.00 & 0 \\ 2.01 & 2.00 & -0.97 & 3.15 & 0 \\ 3.83 & -4.45 & 0.00 & 0.00 & 0 \\ 0.00 & 0.00 & 0.00 & 0.00 & 1 \\ 3.00 & 3.00 & -0.02 & -4.10 & 0 \end{pmatrix} \quad (4)$$

Upon rounding the loadings to the nearest integer, the resulting PC and the correspond-

ing eigenvalues are shown in Table 2. Evidently, the first eigenvector in Eq. (4) suggests that the combination $(ab)^2m^4T^3$ has the largest variability. The second eigenvector implies that the second most-variable combination is $(ab)^2T^3/m^4$. According to the next eigenvector, which has zero eigenvalue, (a/b) is a constant, a consequence of the near-circular orbits in the solar system. The last two eigenvectors, also with zero eigenvalue, imply that $(ab)^3/T^4$ and M are constants. The latter is a consequence of the aforementioned fact that the planets all orbit the same sun in the solar system. Kepler’s law is, therefore, embodied in the penultimate eigenvector. The sample mean of the corresponding principal score is 87.45, and since $a \sim b$, it follows that $\log(a^3/T^2)^2 = 87.45$, i.e., $\log(a^3/T^2) = 87.45/2 = 43.75$. This value is within observational error of $\log(GM/(4\pi^2)) = 42.66$, as expected from Kepler’s law.

As a test of the assumptions of PCA, the scatterplots of the variables (a, b, m, M, T) (after log) are examined. It is found that all of the variables are linearly related, with the exception of M , of course. The pairwise correlation coefficients vary between 0.76 (between a and m) and 1.00 (between a and b). As such, there is no evidence that the linearity assumption is violated.

3.2 Example 2

PCA is often performed on 2-dimensional fields. In image processing circles, the fields are images, i.e., a collection of pixels; in atmospheric sciences PCA is often performed on gridded fields, where the variables are “observed” at each of several thousand grid points across a 2-dimensional spatial lattice. In such applications, the main purpose of PCA is to identify the dominant spatial structures, often called eigenfaces in image processing. Equation discovery, then, requires performing PCA on multiple spatial fields, each corresponding to a different physical variable. For example, two physical variables may be surface temperature and surface pressure. Here, three physical variables are examined: 1) thickness (the vertical distance between two pressure levels), denoted H , 2) mean virtual temperature (the temperature at which a theoretical dry air parcel would have a total pressure and density equal to the moist parcel of air), denoted T_v , and 3) meridional wind speed, denoted V . The first two physical variables are in fact known to follow a “law” known as the hypsometric equation (Wallace and Hobbs 1977):

$$H = (R/g)\log(p_1/p_2)T_v , \quad (5)$$

where $R = 2.87 * 10^2(m^2/(s^2K))$ is the specific gas constant for dry air, $g = 9.8(m/s^2)$ is acceleration due to gravity, and p_1, p_2 are the pressures at the two levels whose thickness is H . Here, the two pressure levels are selected to be 850(HPa) and 500(HPa).

The goal of this example is to demonstrate how PCA can be employed to “discover” the hypsometric equation (dictating H and T_v) from gridded data on H, T_v , and V . The variable V is included in the analysis because in law discovery one does not know what variables are dictated by the law *a priori*. To that end, data are obtained from the Reanalysis project (Kalnay et al. 1996) where all fields are given on a 144×73 grid covering the entire globe. As for the temporal scale of data, focus is placed on the 530 monthly means between Jan 1, 1979 and March 1, 2023. The virtual temperature is not provided in the Reanalysis data base,

and therefore, it is computed from the approximate formula (Doswell and Rasmussen 1994; Glickman 2000) $T_v = T \frac{1+q/0.622}{1+q}$ where T and q are the temperature and specific humidity at a given pressure level, both available in the Reanalysis database. To assure the underlying relationships between the variables are not overwhelmed by the periodic nature of the data, the 12-month period is filtered out using a difference filter, leading to $530 - 12 = 518$ cases. Figure 2 shows the mean (across all 518 months) of the resulting residual fields.

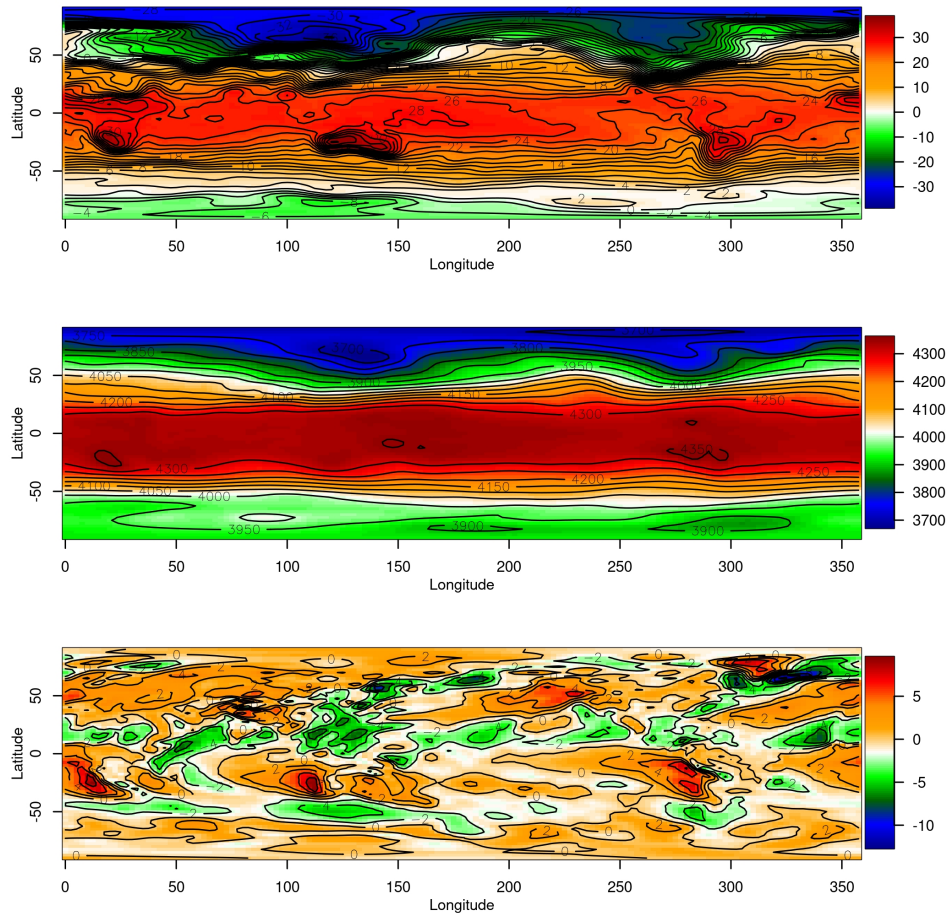


Figure 2. From top to bottom, the mean (across 518 months) of the monthly mean gridded data for virtual temperature (in Centigrade), thickness (in meters), and meridional wind speed (in m/s), after the 12-month period is filtered out.

Performing (S-mode) PCA on a temporal sequence of gridded fields requires “flattening” each image into a vector of inputs (or feature vectors). For example, if PCA is performed on the gridded field of thickness, with 144 grid points along the longitude and 73 grid points along the latitude, then the dimensionality of the input vector is $144 \times 73 = 10,512$. Performing PCA on all three fields combined multiplies the size of the input vector by a factor of 3. Although that number is not prohibitive for modern computing, here each field is cropped to only the northern latitudes from 37.5° to 77.5° . The resulting spatial domain excludes the polar and equatorial regions. Given the 2.5° resolution of the Reanalysis data, this leads to a spatial field with dimensions 144×17 for each of the three physical fields. In

short, the dimensionality of the input vector for the combined PCA is $3 \times 144 \times 17 = 7,344$. The number of cases in the training data is 518, i.e., the number of months in the database. Said differently, the dimension of the data matrix is $518 \times 7,344$, and the correlation matrix has dimensions $7,344 \times 7,344$, leading to $518 - 1$ non-zero eigenvalues.²

The results of the combined PCA are as follows: The screeplot, showing the eigenvalues in decreasing order, is shown in Figure 3; the square root of the eigenvalues is shown on the y-axis, because that quantity measures the standard deviation explained by the corresponding eigenvector. The two curves correspond to the eigenvalues of the covariance matrix (in black) and those of the correlation matrix (in red). Although the results for only the first 200 eigenvectors are shown, the eigenvalues approach zero as the number of eigenvectors approaches 517. The large, filled circles in this figure are discussed in the next subsection.

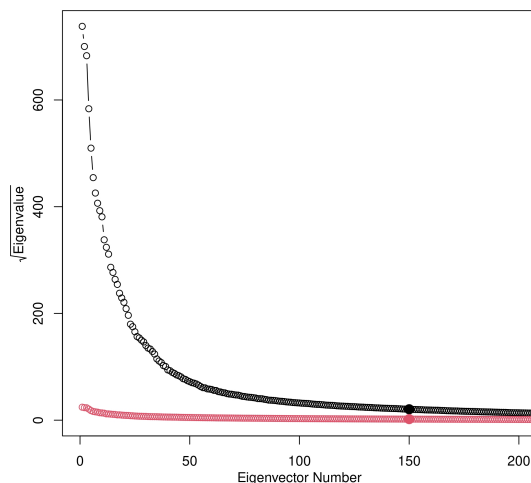


Figure 3. The standard deviation explained by the eigenvectors of the covariance (black) and correlation (red) matrix. The larger, filled circles are addressed in the subsection Eigenvector Selection.

As mentioned previously, in traditional PCA an important question is the smallest number of eigenvectors that adequately explain the majority of the variance. As such, the region of interest is the left side of the screeplot. In the context of equation discovery, however, the region of interest is the right side of the screeplot, because eigenvectors with near-zero eigenvalues define linear combinations of variables that are constant across the cases in the data. The question, then, is how to identify the eigenvector of interest among all of those with near-zero eigenvalues.

²It can be shown that when PCA is performed on p variables and n cases, the number of non-zero eigenvalues is the $\text{minimum}(p, n - 1)$.

3.2.1 Eigenvector Selection

To identify the eigenvector that represents a law, consider the structure of the eigenmatrix, shown in Eq. 6. There are 517 columns corresponding to the eigenvectors with non-zero eigenvalues. There are a total of $3 \times 144 \times 17$ rows corresponding to the three physical fields, with each field consisting of a spatial grid with 144 grid points along the longitude and 17 grid points along the latitude. The goal is to identify the column that represents the hypsometric equation. Also, to assure that none of the three fields dominates an eigenvector simply due to its large variability, henceforth, all eigenvectors are those of the correlation (not covariance) matrix.

$$\begin{pmatrix}
 & e_1 & e_2 & e_3 & \cdots & e_{517} \\
 \hline
 T_v & \cdot & \cdot & \cdot & \cdots & \cdot \\
 & \cdot & \cdot & \cdot & \cdots & \cdot \\
 & \cdot & \cdot & \cdot & \cdots & \cdot \\
 & \vdots & & & & \\
 & \cdot & \cdot & \cdot & \cdots & \cdot \\
 \hline
 H & \cdot & \cdot & \cdot & \cdots & \cdot \\
 & \cdot & \cdot & \cdot & \cdots & \cdot \\
 & \cdot & \cdot & \cdot & \cdots & \cdot \\
 & \vdots & & & & \\
 & \cdot & \cdot & \cdot & \cdots & \cdot \\
 \hline
 V & \cdot & \cdot & \cdot & \cdots & \cdot \\
 & \cdot & \cdot & \cdot & \cdots & \cdot \\
 & \cdot & \cdot & \cdot & \cdots & \cdot \\
 & \vdots & & & & \\
 & \cdot & \cdot & \cdot & \cdots & \cdot
 \end{pmatrix} \cdot \tag{6}$$

Consider the first eigenvector e_1 . Note that each of three segments corresponding to three physical fields can be displayed as an image (an eigenface) with the same dimensions as the original field (Figure 4). In traditional PCA, the spatial structure in these three eigenfaces is employed to identify the dominant oscillations. For example, if PCA were done on surface temperature, then the first column would be an eigenface related to ENSO. Given that PCA is performed on all three variables simultaneously, the correlations between the physical fields is also taken into account. Said differently, if the three fields were totally independent of one another, then the three eigenfaces would be exactly the eigenfaces that one would obtain from PCA performed on the three fields, separately. By the same token, any correlations between the fields will lead to similar eigenfaces. In short, the similarity of the three eigenfaces in Figure 4, is a measure of the association between the underlying physical variables. Similarly, for the other eigenfaces with smaller eigenvalues.

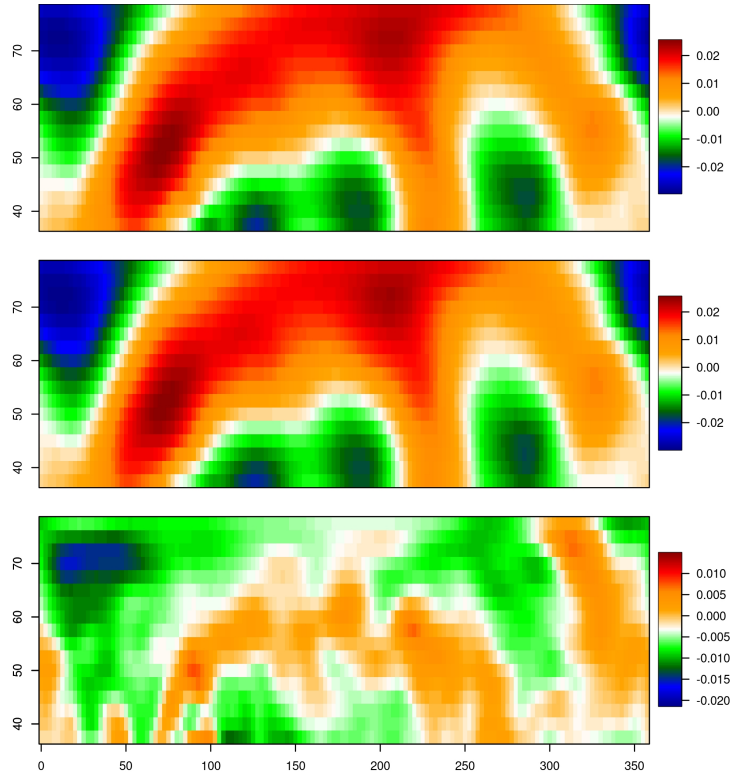


Figure 4. The first eigenface from combined PCA on T_v , H and V .

Although the spatial structure displayed in eigenfaces is important from the perspective of understanding the underlying physical processes, for the present application it is necessary and sufficient to summarize each of the eigenfaces in a way that makes their comparison easier. To that end, Figure 5 displays the loadings of e_1 , i.e., the first eigenvector “prior” to display as the eigenfaces in Figure 4. The numbers on the x-axis are the row number of the eigenmatrix in Eq. 6; the three distinct segments correspond to the three physical fields, and the undulations within each segment are a consequence of the spatial structure in each of the eigenfaces in Figure 4. The advantage of displaying the first eigenface in this fashion is that one can immediately conclude that the first eigenvector is dominated mostly by T_v and H , with the wind variables V having the smallest loadings. This observation can be quantified by the variance of the loadings for each of the three fields, separately. For example, in Figure 5 it is evident that the right-most segment (corresponding to V) has smaller variance across the loadings.

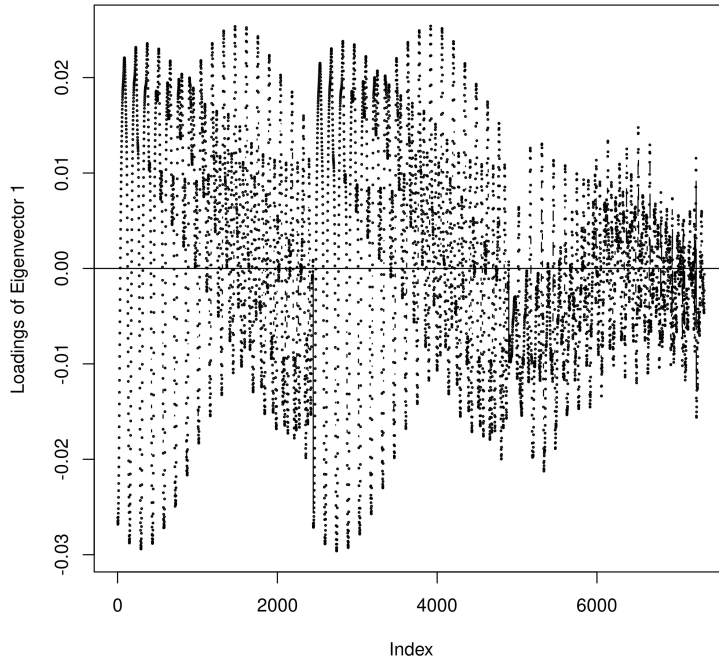


Figure 5. The loadings in the first eigenvector, or equivalently, the first eigenface in Figure 4. The index values (on the x-axis) 1-2448, 2449-4896, and 4897-7344, correspond to T_v , H , and V , respectively.

Figure 6 shows these three variances - actually, standard deviations - for all of the eigenvectors. The black, red, and blue “curves” correspond to T_v , H , and V , respectively. It is important to note that these variances are **across the loadings**, and not the variances that are ordinarily associated with each eigenvector (see Figure 3). Said differently, the former are measures of **spatial** variability, whereas the latter are measures of temporal variability. It is also important to point out that the eigenvectors examined here are eigenvectors of the correlation (not covariance) matrix, which means that the analysis is performed on standardized variables; therefore, any difference in the three “curves” in Figure 6 cannot be due to different temporal variances in the corresponding fields, but rather due to their spatial correlation structure.

Consider eigenvector number 1 in Figure 6. Consistent with Figure 5, T_v and H have comparable variance across the loadings, both larger than the variance of the loadings on V . This pattern is true for the first approximately 20 eigenvectors, beyond which the remaining eigenvectors are dominated by V . The symmetry about the dashed line is a consequence of the fact that each eigenvector is normalized to have a magnitude of 1. Said differently, relatively small loadings for some variables (e.g., T_v and H) must be accompanied by relatively large loadings for other variables (e.g., V). Indeed, the dashed line marks the value of a loading in a normalized eigenvector whose loadings are all equal, i.e., $1/\sqrt{L}$, where $L = 3 \times 144 \times 17$, is the number of loadings in the eigenvector.

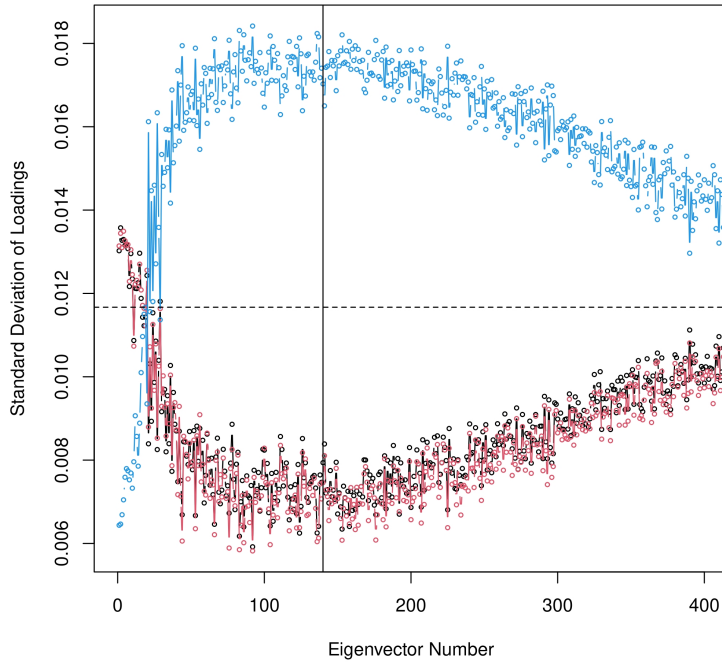


Figure 6. The standard deviation of the loadings of T_v (black), H (red), and V (blue), of each eigenvector.

As mentioned previously, there is no unique eigenvector that corresponds to hypsometric equation; one natural criterion for the selection of that eigenvector is suggested by the pattern of loadings in Figure 6. Given that Figure 6 displays **spatial** variability, it is reasonable to posit that variables relevant to any underlying law must have relatively small spatial variability because the law is expected to be satisfied at all grid points. This criterion immediately rules out V as a variable involved in a law because it displays large spatial variability for all eigenvectors on the right side of the figure. By contrast, T_v and H are ideal candidates for a law. Moreover, the eigenvectors between 100 and 200 have the smallest spatial variability. As such, any one of them is a potential candidate for the “last” eigenvector.

Although, other criteria are proposed in the discussion section, here one can test the validity of this criterion because the underlying law is known to be the hypsometric equation (Eq. 5). To that end, eigenvector number 150 is selected as the “last” eigenvector. Although it is not on the most-right side of the figure, it does have a relatively small eigenvalue (denoted with a filled circle in Figure 3). Using Eq. (3) one can transform a loading (b) to a regression coefficient (β) estimating the coefficient relating T_v to H in Eq. 5. The histogram of the estimate of β at all $144 \times 17 = 2,448$ grid points is shown in the top panel of Figure 7. The theoretical value, $(R/g)\log(850/500) = 15.54(m/K)$ is also shown as the vertical red line. It is evident that the hypsometric law is satisfied at a majority of the grid points. A 2-sided t-test of the null hypothesis that the mean of the estimated β values is equal to the theoretical value leads to a p-value of 0.93 suggesting that there is no evidence from the

data to justify rejecting the null hypothesis. A 95% confidence interval for the true mean is (13.93, 17.01), again consistent with the theoretical value of 15.54.

The bottom panel in Figure 7 displays the spatial map of the estimates of β ; the lack of a coherent spatial structure suggests that the hypsometric equation is satisfied uniformly across the spatial field. All of these results support the proposed criterion for selecting the eigenvector corresponding to the hypsometric equation; other criteria are discussed in the next section.

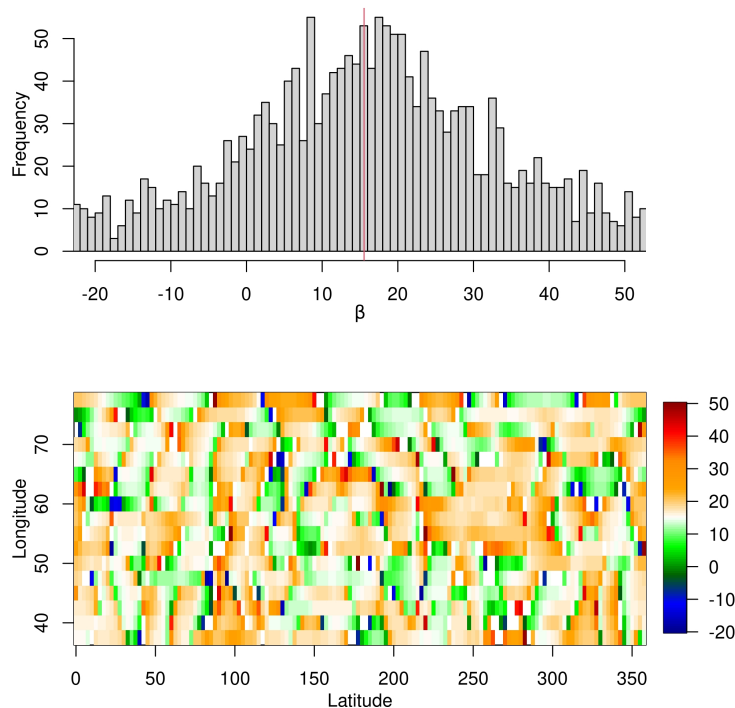


Figure 7. The histogram (top) and the spatial map (bottom) of the estimated β values in Eq. 3.

4 Conclusion and Discussion

It is proposed that PCA can be employed to discover algebraic equations underlying data. Specifically, it is argued that the eigenvectors with the smallest eigenvalues represent combinations of variables that are constant across observations, and therefore, can be useful for equation discovery. Two examples from Physics and Meteorology are employed to demonstrate the proposal.

One of the limitations of the proposed method is that the underlying equations are assumed to be linear in the variables (after transforming the variables into log-space). This is a relatively broad class of functions, including relations of the type $x_0 = \beta_0 + \beta_1 x_1 + \beta_2 x_2 + \dots$, where x_i denote the variables, and β_i are the parameters. It also includes relations of the

type $x_0 = \beta_0 x_1^{\beta_1} x_2^{\beta_2} \dots$, because such a relationship can be transformed to the previous one by taking the logarithm of the variables. However, relationships of the type $x_0 = \beta_0 + \beta_1 x_1^{p_1} + \beta_2 x_2^{p_2} + \dots$, cannot be discovered by PCA. Nonlinear extensions of PCA must be considered for that purpose (Hsieh 2009).

The proposed methodology can be extended in a number of ways, specifically in regards to the criterion for selecting the “last” eigenvector. In the present work, the criterion is based on the spatial variability of the loadings. Ideally, one may have expected the last eigenvector to have near-zero loadings on V , and large loadings on T_v and H . That expectation, however, is based on the assumption that the loadings have no spatial variability, which is simply false. Each of the three fields T_v , H and V have a nontrivial spatial (within-field) correlation structure that prevents any eigenface to have zero variance across grid points.

That said, it is possible to perform the combined PCA on data wherein the T_v , H and V fields have been decorrelated (or “whitened”), individually. The result is that the covariance matrix **within** each field is diagonal, i.e., no spatial correlation. However, an undesirable consequence of this whitening is that the correlations **between** the fields are also affected, possibly altering the underlying law. To remedy this problem it is possible to formulate the eigendecomposition as an optimization problem with a penalty term that attempts to leave the between-field correlations invariant. This idea will be examined at a later time.

Another avenue for future work on the selection of the last eigenvector is based on dimensional analysis, more specifically Buckingham’s π -theorem (Bakarji et al. 2022; Bhaskar and Nigam 1990; Brence, Dzeroski, and Todorovski 2023; Hardtke 2019; Kasprzak, Lysik, and Rybaczuk 1990; Krauss and Wilczek 2014; Xie et al. 2022). This theorem encapsulates the principle of heterogeneity, according to which the laws of nature can be written in terms of dimensionless quantities. Indeed, this theorem can be used to discover the overall structure of Kepler’s third law and the hypsometric equation, on dimensional grounds alone. According to the π -theorem, it can be shown that the combination $\frac{GMT^2}{a^3}$ in Example 1 is the only dimensionless quantity that can be constructed from the variables M , T , a , and the gravitational constant G . As such, the only quantity in Kepler’s third law that cannot be discovered on dimensional grounds is the constant $4\pi^2$. In short, Buckingham’s π -theorem can “explain” why it is possible to discover Kepler’s law empirically at all. As for the hypsometric equation, first, according to the principle of heterogeneity any law (discovered by PCA) must be dimensionless. Second, the π -theorem implies that the only dimensionless quantity that can be constructed from H , T_v , V and the constants R and g , is $\frac{H}{T_v} \frac{g}{R}$; note that the v-component of wind speed (V) does not enter that expression. In other words, based on the π -theorem alone one could have anticipated the PCA results above, namely that the variable V is not relevant to the hypsometric equation, and also that the quantity relevant to the law is $\frac{H}{T_v}$. In short, the π -theorem can aid in determining which eigenvector corresponds to a law. Such considerations are especially important if the data encapsulate multiple laws. Although dimensional analysis has been applied in the context of regression (Shen et al. 2014; Vignaux and Scott 1999), to the knowledge of the authors similar work in PCA has not been done. Work is currently in progress to incorporate the π -theorem into PCA in a formal manner.

In Example 1, Eq. (4) involves a “normalization” that exposes the near-integer values of the loadings. That normalization involves multiplying all the elements in a given eigenvector by some constant. In that example, it is relatively straightforward to determine the value of that constant for each eigenvector. For example, in Eq. (4), all of the elements in the first eigenvector are first divided by the first element, and then multiplied by 2. This leads to first and last loadings that are integers up to 2 decimal places, and a second loading that is an integer to nearly two decimal places (i.e., 2.01); but the third loading (3.83) is relatively far from 4.0. To make this normalization process more objective, one can employ Integer Programming (Lenstra 1983; Sierksma and Zwols 2015), wherein the parameters of optimization are constrained to be integers. Vines (2000) discusses a revision of PCA wherein the loadings are approximately integers. Incorporating these methods into the proposed method will yield a more effective equation discovery approach.

One issue that has not been addressed here is that of sampling variability. For example, when 3.83 is rounded to the integer 4, is that consistent with the level of noise in the data? In other words, it is necessary to provide confidence intervals for the loadings. Then, any integer covered by the confidence interval qualifies as a plausible value. Asymptotic results (Anderson 1984; Ogasawara 2000) and/or bootstrap methods (Davison, Hinkley, and Schechtman 1986) can be employed to supplement the proposed method with measures of confidence.

5 References

1. Anderson, T.W., 1963: Asymptotic Theory for Principal Component Analysis. *Ann. Math. Statist.*, **34** (1), 122-148. DOI: 10.1214/aoms/1177704248
2. Anderson, T. W., 1984: *An introduction to multivariate statistical analysis* (2nd ed.). New York: Wiley.
3. Bakarji, J., J. Callaham, S. L. Brunton, and J. N. Kutz: 2022: Dimensionally consistent learning with Buckingham Pi. *Nat. Comput. Sci.*, **2**, 834–844.
4. Bergen, K. J., P. A. Johnson, M. V. de Hoop, and G. C. Beroza, 2019: Machine learning for data-driven discovery in solid Earth geoscience. *Science*, **363** (6433). DOI: 10.1126/science.aau0323
5. Bhaskar, R., A. Nigam, 1990: Qualitative physics using dimensional analysis. *Artificial Intelligence*, **45** (1–2), 73-111.
6. Bongard, J., and H. Lipson, 2007: Automated reverse engineering of nonlinear dynamical systems. *Proceedings of the National Academy of Sciences*, **104** (24), 9943-9948.
7. Brence, J., S. Dzeroski, and L. Todorovski, 2023: Dimensionally-consistent equation discovery through probabilistic attribute grammars. *Information Sciences*, **632**, 742-756. <https://doi.org/10.1016/j.ins.2023.03.073>

8. Camps-Valls, G., A. Gerhardus, U. Ninad, G. Varando, G. Martius, E. Balaguer-Ballester, R. Vinuesa, E. Diaz, L. Zanna, J. Runge, 2023: Discovering causal relations and equations from data. *Physics Reports*, **1044**, 1-68.
9. Cattell, R. B., 1966: The Scree Test For The Number Of Factors. *Multivariate Behavioral Research*, **1 (2)**, 245-276. doi:10.1207/s15327906mbr0102_10.
10. Chen, B., K. Huang, S. Raghupathi, I. Chandratreya, Q. Du, and H. Lipson, 2022: Automated discovery of fundamental variables hidden in experimental data, *Nature Computational Science*, **2**, 433-442.
11. Davison, A.C., D.V. Hinkley, and E. Schechtman, 1986: Efficient bootstrap simulation. *Biometrika*, **73**, 555-566.
12. Dmitrienko, A., C. Chuang-Stein, R. B. D'Agostino, 2007: *Pharmaceutical Statistics Using SAS: A Practical Guide*. SAS Institute. 380 pp. ISBN 978-1-59994-357-2.
13. Doswell, C. A., III and E. N. Rasmussen, 1994: The Effect of Neglecting the Virtual Temperature Correction on CAPE Calculations, *Wea. Forecasting*, **9 (4)**, 625-629. [https://doi.org/10.1175/1520-0434\(1994\)009;0625:TEONTV;2.0.CO;2](https://doi.org/10.1175/1520-0434(1994)009;0625:TEONTV;2.0.CO;2)
14. Elmore, K. L., and M. B. Richman, 2001: Euclidean Distance as a Similarity Metric for Principal Component Analysis. *Mon. Wea. Rev.*, **129 (3)**, 540-549. [https://doi.org/10.1175/1520-0493\(2001\)129;0540:EDAASM;2.0.CO;2](https://doi.org/10.1175/1520-0493(2001)129;0540:EDAASM;2.0.CO;2)
15. Gertler, J., and J. Cao, 2005: Design of optimal structured residuals from partial principal component models for fault diagnosis in linear systems. *Journal of Process Control*, **15 (5)**, 585-603.
16. Glickman, T. 2000: Glossary of meteorology. American Meteorological Society. ISBN: 9781878220349. https://glossary.ametsoc.org/wiki/Virtual_temperature#:~:text=Hence%20the%20v
17. Grundner, A., T. Beucler, P. Gentine, V. Eyring, 2023: Data-Driven Equation Discovery of a Cloud Cover Parameterization, arXiv preprint arXiv:2304.08063
18. Hardtke, J-D., 2019: On Buckingham's π -Theorem. <http://arxiv.org/abs/1912.08744v1>
19. Hoerl, R. W., R. D. Snee, R. D. De Veaux, 2014: Applying statistical thinking to 'Big Data' problems. *WIREs Computational Statistics*, **6 (4)**, 211-312. https://doi-org.offcampus.lib.washington.edu/10.1002/wics.1306open_in_new
20. Hotelling, H. (1933). Analysis of a complex of statistical variables into principal components. *Journal of Educational Psychology*, 24(6), 417-441. <https://doi.org/10.1037/h0071325>
21. Hsieh, W.W., 2009: Nonlinear Principal Component Analysis. In: Haupt, S.E., Pasini, A., Marzban, C. (eds) *Artificial Intelligence Methods in the Environmental Sciences*. Springer, Dordrecht. https://doi.org/10.1007/978-1-4020-9119-3_8
22. Huang, B., 2001: Process identification based on last principal component analysis. *Journal of Process Control*, **11**, 19-33.

23. Ibebuchi, C. C., M. B. Richman, 2023: Circulation typing with fuzzy rotated T-mode principal component analysis: methodological considerations. *Theoretical and Applied Climatology*, **153**, 495-523.
24. Jolliffe I. T. 2002: *Principal Component Analysis*, 2nd edn. New York, NY: Springer-Verlag. 518 pp.
25. Jolliffe I. T., J. Cadima, 2016: Principal component analysis: A review and recent developments. *Phil. Trans. R. Soc. A*, **374**. Article ID: 20150202. <http://dx.doi.org/10.1098/rsta.2015> site Jolliffe's book on pca, and their own section 3c for an image analysis example.
26. Kalnay E., M. Kanamitsu, R. Kistler, W. Collins, D. Deaven, L. Gandin, M. Iredell, S. Saha, G. White, J. Woollen, Y. Zhu, M. Chelliah, W. Ebisuzaki, W. Higgins, J. Janowiak, K. C. Mo, C. Ropelewski, J. Wang, A. Leetmaa, R. Reynolds, Roy Jenne, and Dennis Joseph, 1996: The NCEP/NCAR 40-Year Reanalysis Project. *BAMS*, **77(3)**, 437-472. [https://doi.org/10.1175/1520-0477\(1996\)077;0437:TNYRP;2.0.CO;2](https://doi.org/10.1175/1520-0477(1996)077;0437:TNYRP;2.0.CO;2)
27. Kamath, C., 2001: On Mining Scientific Datasets. In: Grossman, R.L., Kamath, C., Kegelmeyer, P., Kumar, V., Namburu, R.R. (eds) *Data Mining for Scientific and Engineering Applications*. Massive Computing, vol 2. Springer, Boston, MA. https://doi.org/10.1007/978-1-4615-1733-7_1
28. Kasprzak, W., B. Lysik, and M. Rybaczuk, 1990: *Dimensional Analysis in the Identification of Mathematical Models*, 204 pp. <https://doi.org/10.1142/1162>
29. Kratzert, F., D. Klotz, G. Shalev, G. Klambauer, S. Hochreiter, and G. Nearing, 2019: Towards learning universal, regional, and local hydrological behaviors via machine learning applied to large-sample datasets. *HESS*, **23 (12)**, 5089-5110. <https://doi.org/10.5194/hess-23-5089-2019>
30. Krauss, L.M. and F. Wilczek, 2014: Using cosmology to establish the quantization of gravity. *Phys. Rev. D*, **89**, 047501.
31. Kurgan, L., and P. Musilek, 2006: A survey of Knowledge Discovery and Data Mining process models. *The Knowledge Engineering Review*, **21 (1)**, 1-24.
32. Langley, P. 1981: Data-driven discovery of physical laws. *Cognitive Science*, **5 (1)**, 31-54. [https://doi.org/10.1016/S0364-0213\(81\)80025-0](https://doi.org/10.1016/S0364-0213(81)80025-0)
33. Lenstra, H. W., 1983: Integer Programming with a Fixed Number of Variables. *Mathematics of Operations Research*, **8 (4)**, 538-548. doi:10.1287/moor.8.4.538.
34. Lorenz, E. N. 1956. Empirical orthogonal functions and statistical weather prediction, Scientific Report 1, Statistical Forecasting Project. Massachusetts Institute of Technology Defense Doc. Center No. 110268, 49 pp. <http://muenchow.cms.udel.edu/classes/MAST811/Lorenz>

35. Marzban, C., and U. Yurtsever, 2017: On the Shape of Data. Paper presented at the 15th Conference on Artificial Intelligence, at the 97th American Meteorological Society Annual Meeting, Seattle, Jan. 22-26.
36. Marzban, C., and U. Yurtsever 2011: Baby Morse theory in data analysis. Paper at the workshop on Knowledge Discovery, Modeling and Simulation (KDMS), held in conjunction with the 17th ACM SIGKDD Conference on Knowledge Discovery and Data Mining, San Diego, CA., August 21-24.
37. North, G. R., T. L. Bell, R. F. Cahalan, and F. J. Moeng, 1982: Sampling Errors in the Estimation of Empirical Orthogonal Functions. *Mon. Wea. Rev.*, **110** (7), 699-706. DOI: [https://doi.org/10.1175/1520-0493\(1982\)110;0699:SEITEOj2.0.CO;2](https://doi.org/10.1175/1520-0493(1982)110;0699:SEITEOj2.0.CO;2)
38. Ogasawara, H., 2000: Standard errors of the principal component loadings for unstandardized and standardized variables. *British Journal of Mathematical and Statistical Psychology*, **53**, 155-174.
39. Rolle, J.-D., 2002: Notes about the last principal component. *Appl. Math. Comput.*, **126**, 231-241.
40. Schmidt, M., and H. Lipson, 2009: Distilling Free-Form Natural Laws from Experimental Data. *Science*, **324**, 81-85.
41. Shen, W., T. Davis, D. K. J. Lin, and C. J. Nachtsheim, 2014: Dimensional Analysis and Its Applications in Statistics. *Journal of Quality Technology*, **46** (3), 185-198.
42. Sierksma, G, and Y. Zwols, 2015: *Linear and Integer Optimization: Theory and Practice*. CRC Press. ISBN 978-1-498-71016-9.
43. Song W., L. Shi, X. Hu, Y. Wang, and L. Wang, 2023: Reconstructing the Unsaturated Flow Equation From Sparse and Noisy Data: Leveraging the Synergy of Group Sparsity and Physics-Informed Deep Learning. *Water Resources Research*, **59**(5), 1-24. <https://doi.org/10.1029/2022WR034122>
44. Vignaux, G. A., and J. L. Scott, 1999: Simplifying Regression Models Using Dimensional Analysis. *The Australian and New Zealand Journal of Statistics*, **41** (1), 31-42.
45. Vines, S.K., 2000: Simple principal components. *Appl. Statist.*, **49** (4), 441-451.
46. Wallace, J. M., and P. V. Hobbs, 1977: *Atmospheric Science: An Introductory Survey*. Academic Press.
47. Wang, X.Z., 1999: Data mining and knowledge discovery for process monitoring and control. *Advances in Industrial Control*, 1-251, ISBN 1-85233-137-2 .
48. Wilks, D. S., 2016: Modified “Rule N” Procedure for Principal Component (EOF) Truncation. *Journal of Climate*, **29** (8), 049-3056. <https://doi.org/10.1175/JCLI-D-15-0812.1>

49. Wilks, D. S., 2019: *Statistical Methods in the Atmospheric Sciences*, Fourth Edition, Elsevier. <https://doi.org/10.1016/C2017-0-03921-6>
50. Xie X., A. Samaei, J. Guo, W. K. Liu, and Z. Gan, 2022: Data-driven discovery of dimensionless numbers and governing laws from scarce measurements. *Nature Communications*, **13**, 7562.
51. Xu, W., and M. Stalzer, 2019: Deriving compact laws based on algebraic formulation of a data set. *Journal of Computational Science*, **36**. <https://doi.org/10.1016/j.jocs.2019.06.006>
52. Yu, S., and J. Ma, 2021: Deep learning for geophysics: Current and future trends. *Reviews of Geophysics*, **59**. <https://doi.org/10.1029/2021RG000742>
53. Zanna, L., and T. Bolton, 2020: Data-driven equation discovery of ocean mesoscale closures. *Geophys. Res. Lett.*, **47**, e2020GL088376, <https://doi.org/10.1029/2020GL088376>.
54. Zhang, S., and G. Lin, 2018: Robust data-driven discovery of governing physical laws with error bars. *Proceedings of the Royal Society A*, **474**. <https://doi.org/10.1098/rspa.2018.0305>
55. Zlobina, A.G., and I. V. Zhurbin, 2020: Applying a Principle Component Analysis to Search for Objects on Historical Territories by the Spectral Brightness of Vegetation. *J. Phys.: Conf. Ser.*, **1611**, 1-7. doi:10.1088/1742-6596/1611/1/012064